EPiC Series in Technology
Volume 4, 2026, Pages 90–103
Proceedings of The 11th International Conference on Tribology in Manufacturing Processes & Advanced Surface Engineering

# Mixed Lubrication Regime Modelling in Cold Strip Rolling: Toward a More Complete Physical Description of the Boundary Component

Pierre Montmitonnet[1], Imène Lahouij[1], Cynthia Elhajj[1,2], Geoffroy Bouillet[1,3], Linh Phuong Luong[2], Jean-Denis Mithieux[2], Alexandre Barthélémy[3], Ariane Viat[3], Vincent Duhoux[3]
[1] MINES Paris PSL, CEMEF, CNRS UMR 7635, Sophia Antipolis, France
[2] Aperam R&D, Isbergues, France
[3] Constellium C-TEC, Voreppe, France
Pierre.montmitonnet@minesparis.psl.eu, imene.lahouij@minesparis.psl.eu, cynthia.elhajj@minesparis.psl.eu, geoffroy.bouillet@minesparis.psl.eu, linh.luong@aperam.com, jeandenis.mithieux@aperam.com, alexandre.barthelemy@constellium.com, Ariane.viat@constellium.com, Vincent.duhoux@constellium.com

**Abstract**

Predictive models are needed to design cold strip rolling pass schedules, investigate process problems and product quality. Due to the huge and complex impact of friction on this process, accurate friction models are necessary. The forward slip e.g. depends not only on average friction, but also on its space-distribution; friction also varies in time, e.g. accelerations and decelerations result in large variations of force, torque and forward slip during transients, which need to be considered in the presetting of stands.

Describing space- and time-variations of friction necessitates including the scale at which physical and chemical phenomena vary and determine friction, i.e. the microscale. This paper describes our latest efforts to enrich our mixed lubrication modelling of cold rolling, in search for a more accurate description of what is going on at asperity scale in the strip-roll interface. It involves a macroscale description of the interface temperature profile, criteria for lubricant additive desorption, for asperity scale adhesion and metallic transfer film formation, major phenomena which impact the degree of ploughing friction. Principles of the model are recalled, and the theoretical results are confronted with experiments on a high-speed laboratory rolling mill.

# 1 Introduction and bibliography

Tribology of lubricated mechanical systems generally couples many different phenomena, with the related technologies and scientific fields: mechanics (solids and fluids), heat transfer, materials science and surface science for additive adsorption and, if some kind of seizure occurs, for adhesion. Moreover, several spatial scales must be covered, e.g. mechanics at the system scale as well as the contact size scale and the roughness scale.

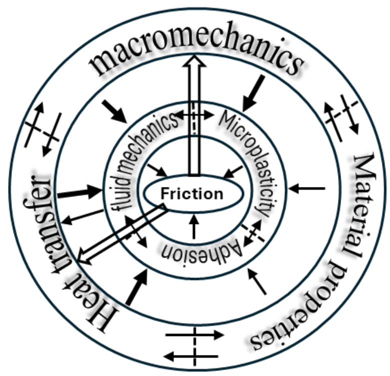


**Figure 1**: Description of the multi-physical and multiscale coupling in mixed lubrication modelling

This paper summarizes a comprehensive model of cold strip rolling. The rolling process is no exception to the above rule of Figure 1. More specifically, rolling is most of the time performed in the mixed lubrication regime, with either oils or emulsions. The reason is that enough friction must be ensured to force entrainment of the strip: friction is the driving force of this process. This means that oil viscosity is chosen such that lubricant film thickness $h_t$ ~ 100 to 300 nm, often well below the combined roughness (100 to 500 nm $R_q$). Therefore, Tallian's number $h_t/R_q$ ~ 1 or even less, which gives a major role to the boundary regime and the chemistry of the additives of the lubricant.

This is why cold rolling lubrication has been modelled in the mixed regime as soon as Tsao & Sargent (1977) who introduced the partition of pressure and friction stress between solid contact spots and pressurized fluid lubricant (see Figure 4 and Eq. (6) below). The locally averaged pressure was provided by a standard strip rolling model by the Slab Method (Von Karman, 1925), the solution of the Reynolds' equation gave the local oil pressure. The pressure left to be carried by asperities gave the local fractional real contact area and the local film thickness. This approach was refined in the next decade by Sutcliffe & Johnson (1990) and Sheu & Wilson (1994), using specifically developed models of asperity flattening. The key point is that the latter include microplasticity / macroplasticity coupling (Sutcliffe, 1988) (Wilson & Sheu, 1988), i.e. the observation that asperities need less pressure to be plastically deformed when they lie on a plastically deforming (elongating) bulk. Following Patir & Cheng (1979), they also introduced flow factors in Reynolds' equation to consider the impact of roughness on lubricant flow (hindrance to pressure gradient flow component, enhanced transport by the solids velocity term). Flow factors were later on adapted to $h_t/R_q$ < 1 by Wilson & Marsault (1998). Marsault (1998) gathered all these elements in a complete rolling model with the friction stress calculated locally by the above lubrication models. He was followed by Carretta (2014) and Boemer (2020). Note for completeness that similar or slightly different approaches of mixed lubrication in strip rolling were developed a.o. by Rasp & Häfele (1998), Qiu et al. (1999) or more recently and based on similar ideas, Wu et al. (2016), Li et al. (2019) and Jacobs et al. (2025).

Such models allow the effect of all rolling parameters to be described and understood, not only roll diameter, thickness reduction, mechanical properties of the metal and strip tensions as in "standard" strip rolling models, but also roll speed, oil viscosity law, strip and roll roughness descriptors. However, the solid-solid contact ("plateaus") is described by a single friction coefficient or factor, which does not represent the diversity of the boundary lubrication reigning there, so that in the end it plays the role of a fitting coefficient. The ambition of this paper is to bridge a gap with known phenomena which dominate boundary lubrication: desorption of lubricant additive and eventually formation of a thick, tribologically detrimental metal transfer layer on the roll ("roll coating"), changing its surface properties and resulting in much increased friction. As these phenomena are thermally activated ones, as shown by Rizoulières (2000) or Montmitonnet et al. (2000), a thermal model of roll, strip and interface has been developed and is sketched in the following. Based on a temperature criterion inspired by Azushima (1987), an adhesive transfer evolution model has been implemented based on ideas in Kitano et al. (2016). These physical models of the boundary contact spots have been coupled to a mixed lubrication model according to the principles first described in Tsao & Sargent (1977), Sutcliffe & Johnson (1990), Sheu & Wilson (1994) and Marsault (1998). This comprehensive lubrication model has been implemented in an existing cold strip rolling model including elastic roll deformation. In the following, the basic principles of all the bricks of the model are briefly described, then the impact of roll speed and thickness reduction on friction is described as an example of application. As a second application, prediction of adhesion in stainless steel cold rolling is compared to (Rizoulieres, 2000) experiments on a laboratory, high-speed cold strip rolling mill.

# 2 Thermal-mechanical model

## 2.1 1D strip + roll mechanical model

The plastic deformation of the strip is described by the Slab Method (von Karman, 1925), which consists in assuming stresses independent of the thickness direction and in neglecting shear stress components in the constitutive model, so that the principal stress directions coincide everywhere with the rolling axes, Rolling Direction (RD, x), Normal Direction (ND, y) and Transverse Direction (TD, z). Plane strain (x,y) is assumed. These simplifications constitute a standard treatment for wide, thin strips such as in cold rolling. The equilibrium equations are thus simplified into:

$$\frac{d(\sigma_{xx}.t)}{dx} = -p\frac{dt}{dx} - 2\tau \qquad (1)$$

where $\sigma_{xx}(x)$ is the longitudinal stress in the Rolling Direction, $t(x)$ the strip thickness, $p(x)$ and $\tau(x)$ the normal and friction contact stresses respectively. The elastic-plastic constitutive model chosen is the Prandtl and Reuss one (additiveness of elastic and plastic strain rate, hypoelastic elastic strain-rate – stress rate relationship, von Mises yield criterion and associated flow rule). Together with the equilibrium equations, this gives a set of Ordinary Differential Equations (ODEs) solved by a $4^{th}$-order Runge-Kutta (RK4) technique. Friction is described by Coulomb's law.

Roll elastic deformation is treated in plane strain $(x,y)$ as well, using an elastic foundation model described in Johnson (1987), which considers only vertical displacements of the roll surface. The complex stress profile from the Slab Method is discretized and the additivity rule is applied in the elastic solution, resulting in a matrix method. The solution (roll surface displacement in the $(x,y)$ plane) iteratively modifies the roll profile $y_{roll}(x)$ used in (1) to determine $t(x)$. At each iteration, the roll centerline is shifted vertically to maintain a constant exit strip thickness (i.e. the requested thickness reduction). In the case of severe roll deformation, it is extremely important to apply an efficient relaxation scheme between roll and strip models, in general with an adaptive relaxation coefficient.

In case of moderate loads, Hitchcock's model (1935) is used as a simpler and less costly alternative: the roll is assumed to deform elastically into a circular profile with larger diameter, using Hertz' contact solution; to do so, the normal stress profile is approximated by an elliptic one with the same integral.

## 2.2 2D strip + roll thermal model

The strip temperature field is obtained by solving a steady state heat transfer equation:

$$u(x).\frac{\partial T}{\partial x} + v(x,y).\frac{\partial T}{\partial y} = a_{strip}\left(\frac{\partial^2 T}{\partial x^2} + \frac{\partial^2 T}{\partial y^2}\right) + 0.9\,\frac{\sigma_0(x).\dot{\bar{\varepsilon}}}{\rho C_{strip}} \quad (2)$$

Temperature $T(x,y)$ (hereafter in Celsius) is assumed independent from $z$ (TD) in accordance with the mechanical model assumptions. Velocity components for the advection term are noted $u$ and $v$. $a_{strip}$, $\rho$ and $C_{strip}$ are the strip metal thermal diffusivity, volumic mass and specific heat respectively. The yield stress $\sigma_0(x)$ may be updated for strain-hardening, strain-rate sensitivity $\dot{\bar{\varepsilon}}(x)$ coming from the mechanical model, and temperature. The Taylor-Quinney coefficient is taken equal to 0.9 as usual. Boundary Conditions (BC) consist in a given inlet temperature $T_0$, symmetry $\partial T/\partial y = 0$ at mid-thickness $y = 0$, and a Heat Transfer Coefficient (HTC) $h_{contact}$ at roll contact ($\phi$ is the heat flux and $T_s$ the surface temperature):

$$\phi(x) = h_{contact}.\left(T_{s,strip}(x) - T_{s,roll}(x)\right) \quad (3)$$

For the roll, the thermal model is written in cylindrical coordinates $(r,\theta)$. Temperature $T(r,\theta)$ is assumed independent from $z$ (TD). The steady state form of the Heat Transfer Equation writes:

$$\frac{\partial^2 T}{\partial r^2} + \frac{1}{r}\frac{\partial T}{\partial r} + \frac{1}{r^2}\frac{\partial^2 T}{\partial \theta^2} = \frac{\omega}{a_{roll}}\frac{\partial T}{\partial \theta} \quad (4)$$

where $\omega$ is the roll angular velocity and $a_{roll}$ is the roll metal thermal diffusivity. As for BCs, flux $\phi(\theta)$ is described by (3) for the strip-roll contact area. In the following, a correlation given by Mikic (1974) and Tseng (1999) is used throughout (other forms can easily be implemented):

$$h_{contact}(x) = 3800.\frac{2\lambda_{strip}.\lambda_{roll}}{\lambda_{strip}+\lambda_{roll}}\,.Ra^{-0.257}.\left(\frac{p(x)}{p(x)+3\sigma_0(x)}\right)^{0.94} + \frac{\lambda_{lub}}{h_t(x)}.\left(1 - A(x)\right) \quad (5)$$

λ's are thermal conductivities, Ra is the combined Centre Line Average (CLA) roughness of roll and strip, in µm $\left(Ra = \sqrt{Ra_{strip}^2 + Ra_{roll}^2}\right)$, $h_t$ is the lubricant film thickness and A the fractional real contact area. The last two variables are given by the lubrication model to be presented next; they evidence the feedback from the lubrication model to the heat transfer model.

Angular distributions $h(\theta)$ can be used to model convective exchanges with air as well as roll cooling and lubricant jets, and the contact with back-up rolls. For convection with fluids, standard formulae relating Nüsselt's number $Nu = hR/\lambda$ to Reynolds' and Prandtl's numbers are used, accounting for either laminar or turbulent fluid flows (see e.g. Sacadura (2015)).

Both strip and roll models are solved by the Finite Difference Method (FDM). In both cases, due to the high Peclet number, upwind formulations must be used. As shown e.g. by Patula (1981), beyond a thin layer ~ $\sqrt{2\,a_{roll}/\omega}$ (typically ≤ 1 mm), $T(r,\theta)$ becomes a constant $T_{core}$ to a very good approximation. Therefore, meshing is restricted to a thickness ~$10.\sqrt{2\,\omega/a_{roll}}$ and an inner BC $\partial T/\partial r = 0$ allows retrieving $T_{core}$ (Figure 2).

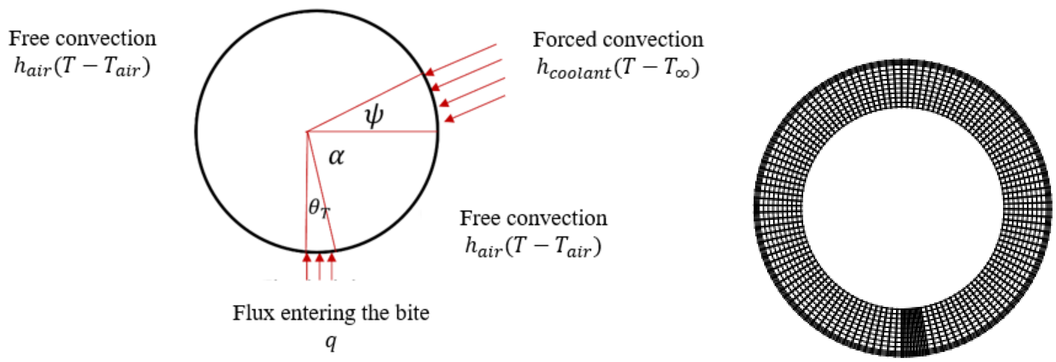


**Figure 2**: Boundary Conditions (left) and meshing (right) of the roll temperature model

An alternative, transient form of the Heat Transfer Equation for roll temperature is used in the following to feed the temperature criterion of adhesive transfer layer development:

$$\frac{\partial T}{\partial t} = a_{roll}\left(\frac{\partial^2 T}{\partial r^2} + \frac{1}{r}\frac{\partial T}{\partial r}\right) \tag{5}$$

Here, thanks to the very high Peclet number, the $\theta$-derivatives are omitted and replaced by the rotation at angular velocity $\omega$ of the 1D-mesh of the roll in the $h_{contact}(\theta)$ field.

# 3 Mixed regime lubrication model

Figure 3 represents schematically the macroscale and the microscale contact configurations. At the microscale, the rolling pressure is supported partly by direct asperity contact spots (fraction $A$, pressure $p_a$, friction stress $\tau_a$), the rest by the fluid pressure (on fractional area $1-A$, pressure $p_b$, friction $\tau_b$).

## 3.1 Stress partition equations

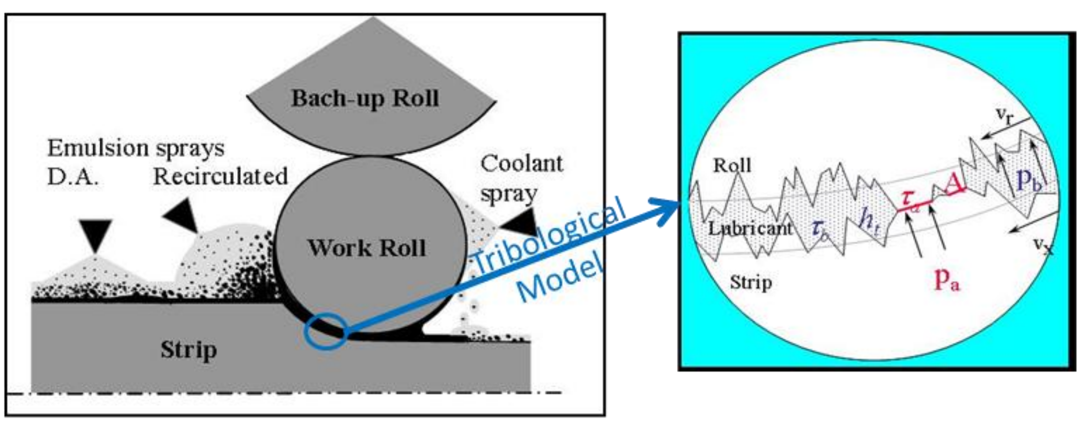


**Figure 3**: Schematic description of contact between rough surfaces under mixed lubrication.

In a mechanical homogenization perspective, normal and tangential stresses are averaged over a length much larger than the distance between asperities, but much smaller than the roll contact length. The weights are given by the respective proportions of "plateaus" and "valleys", $A$ and 1-$A$.

$$p(x) = (1 - A(x)).p_b(x) + A(x).p_a(x) \tag{6a}$$
$$\tau(x) = (1 - A(x)).\tau_b(x) + A(x).\tau_a(x) \tag{6b}$$

Pressure $p$ coming from the thermo-mechanical rolling model is thus distributed between plateaus and valleys according to their respective "rigidities", the dependence of which on $A$ and $h_t$ are determined in the next subsections. The lubrication model feedback to the rolling model is a weighted average of fluid shear stress $\tau_b$ and solid (boundary) friction stress $\tau_a$, the determination of which is also detailed in the following.

## 3.2 Lubricant flow model

The load-bearing capacity of the fluid is described as usual by Reynolds' equation; again, a steady-state and plane-strain version is used. It is written below after a first integration which introduces an important physical unknown, the volume of lubricant going through the roll bite per unit time, $Q_{lub}$ (it is x-independent, its conservation is the fundamental meaning of Reynolds' equation):

$$\varphi_p(h_t).\frac{h_t^3}{12\eta}.\frac{dp_b}{dx} = \frac{V_x+V_{roll}}{2}.h_t + \frac{V_x-V_{roll}}{2}.R_q.\varphi_s(h_t) - Q_{lub} \tag{7}$$

$\eta(T,p_b)$ is the lubricant viscosity, $v_{roll} = \omega R$ the tangential roll velocity, $v_x(x) = v_{roll}.t_N/t(x) = v_{roll}.(1+S_f).t_{out}/t(x)$ is the local strip velocity along RD. $t_N$ is the thickness at the neutral point, $t_{out}$ the known exit thickness and $S_f = (v_{out}-v_{roll})/v_{roll}$ is the forward slip, an important characteristic of strip rolling since rolling does not impose a strict exit strip velocity. $R_q$ is the combined Root Mean Square (RMS) roughness of strip and roll. $\varphi_p$ and $\varphi_s$ are the pressure and shear flow factors, which represent the effect of roughness respectively on the Poiseuille term (pressure gradient) and the Couette term (entrainment by solid velocity). They are expressed as functions of $h_t/R_q$ and of a roughness anisotropy factor, the Peklenik number (Wilson & Marsault (1998), Marsault (1998), Boemer (2020)).

Reynolds equation is one more ODE which is added to the previously mentioned set (strip rolling model, section 2.1), the solution being performed in common. $Q_{lub}$ being an unknown, an iterative shooting method is needed with the convergence condition $p_b = p = 0$ at the exit point.

Finally, fluid friction is calculated at each position by Newton's equation of viscosity:

$$\tau_b(x) = \eta.\frac{\partial u_{lub}(x,y)}{\partial y} \approx \eta\big(T(x),p(x)\big).\frac{v_{strip}(x)-v_{roll}}{h_t(x)} \tag{8}$$

## 3.3 Asperity interaction model

It has long been observed that asperities are flattened more easily on a plastically deforming metal that on an elastic material (e.g. "dead" zones in metal forming). Experiments by Sutcliffe (1988) or Wilson & Sheu (1988) have evidenced and quantified this effect. Based on this, they developed models coupling micro- with macro-plasticity. One of them is sketched hereafter, but other ones can be easily plugged in. It is based on velocity fields described in Figure 4, from which, using the Upper Bound Theorem, the plastic power is deduced, hence the load to apply on the asperity to maintain plastic flow. This micro-macro coupling is represented by the factor:

$$\mathrm{E_p} = -\frac{\dot{\varepsilon}_{\mathrm{x}} l}{\mathrm{v_a}+\mathrm{v_b}} \tag{9}$$

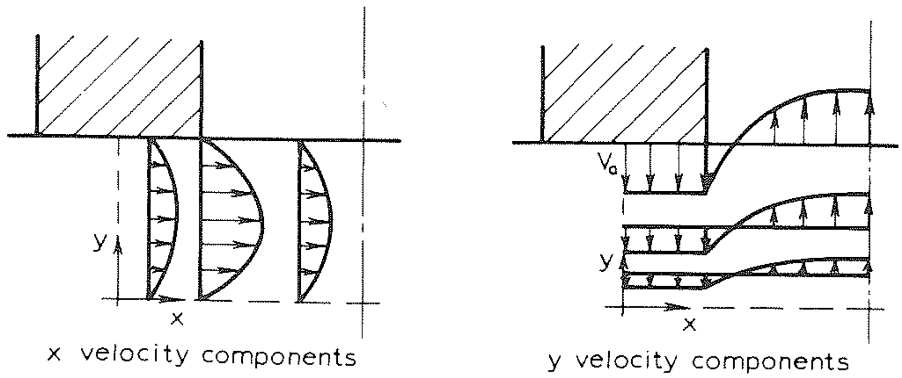


**Figure 4**: Longitudinal, periodic asperity flattening model (Wilson & Sheu (1988)). The punch (dashed) represents the roll surface which pushes down the asperity material; by incompressibility, the material in the neighbouring valley moves up.

where $\dot{\varepsilon}_x = \partial v_x / \partial x$ is the strip macroscopic plastic strain rate, whereas $(v_a+v_b)/l$ approximates the micro-strain rate during asperity deformation. $l$ is the average distance between asperities, a fundamental roughness parameter describing horizontal spread, $v_a$ and $v_b$ the asperity top flattening velocity and the valley bottom upheaval velocity, respectively (Figure 4).

The resistance to flattening is represented by the "apparent hardness" $H_a$, which depends on the present fractional contact area $A$ (the ratio of plateau widths to $l$ in this periodic model), the micro-macro factor $E_p$ and the lubricant pressure, which, applied on the flanks of the asperity, backs it up against plastic deformation (a multiaxial, plasticity criterion effect). Hence, the use of the term $p_a$-$p_b$:

$$H_a = \frac{p_a - p_b}{k_0} = H_a(A, E_p) \tag{10}$$

($k_0 = \sigma_0/\sqrt{3}$ is the yield stress in pure shear). As an example (used in the following), Wilson & Sheu (1988) performed an extensive application of their model to a large number of configurations with longitudinal roughness lays, and fitted the results by:

$$H_a = \frac{p_a - p_b}{k_0} = 2\left(\left(0.515 + 0.345A - 0.86A^2\right).E_p + \frac{1}{2.571 - A - A.\ln(1-A)}\right)^{-1} \tag{11}$$

Based on the definition of the height distribution function $f(h)$ of the roughness, $dA/dh = f(h)$ and the evolution rate of $A$ in the roll bite can be calculated:

$$\frac{dA}{dx} = \frac{\dot{\varepsilon}_x l}{v_x E_p}.f(h) = -\frac{v_a + v_b}{v_x}.f(h) \tag{12}$$

This is another ODE to be coupled with the existing set. Finally, boundary friction stress is obtained:

$$\tau_a = \mu_a.p_a \text{ (Coulomb) or } \tau_a = m_a.\frac{\sigma_0(x)}{\sqrt{3}} \text{ (friction factor)} \tag{13}$$

The boundary friction coefficient or factor may be chosen based on the ploughing theory of friction, knowing the local roughness (Jacobs, 2025). The purpose of the next section is to propose a way to describe its *evolution* once a severity criterion of the boundary regime is met.

## 3.4 Adhesion model and friction dependence

In stainless steel cold strip rolling, Azushima (1987) showed that the occurrence of adhesive transfer and the resulting strip surface quality degradation are strongly connected to temperature. Namely, it occurred in his tests when the strip surface temperature, measured just after the exit of the roll bite, exceeded ~150°C; the roll temperature in the same tests was ~100°C. These values are close to the known desorption temperature range of the oiliness additives (friction modifiers) contained in the lubricating oils. This temperature dependence was confirmed by Rizoulières (2000). Conversely, adhesive transfer considerably increases frictional dissipation, hence temperature, as schematically pictured in Figure 1. It is therefore natural to establish an adhesion start criterion on the local temperature. Another necessary condition is the boundary character of the lubrication regime, since adhesion will not start under thick film conditions. The chosen criterion therefore writes:

$$\frac{h_t}{R_q} < 1 \ \text{ and } \ T(x) > T_{crit} \tag{14}$$

Once started, the evolution of the coverage $\theta_{adh}$ of the roll surface by the adhesive transfer layer depends (i) on temperature (adhesion is all the faster and stronger as temperature is higher); (ii) on contact pressure which damages protective oxides; and (iii) on surface expansion which brings reactive metal to the contact. The sliding length is another potentially important factor, not included yet.

From a quantitative point of view, a relation for the coverage $\theta_{adh}(t)$ proposed by Kitano et al. (2016) has been used here:

$$d\theta_{adh} = K.(1-\theta_{adh})f(p,\xi)e^{-\frac{\alpha}{T}}.ds \tag{15}$$

Where $ds = Rd\Phi$ is the length element, $p$ the pressure, $T$ the temperature, $\xi$ surface expansion. $K$ and $\alpha$ are properties of the strip-roll-lubricant interface. This relation needs temperature T(x,t), hence based on the time-marching version of the thermal model, eq.(5).

Again, it is straightforward to substitute Eq. (14-15) with any other relation better adapted to specific cases. Note e.g. that eq.(15) does not account for the reversibility of the transfer, which has been shown by Rizoulières (2000) (see also Montmitonnet et al. (2000)).

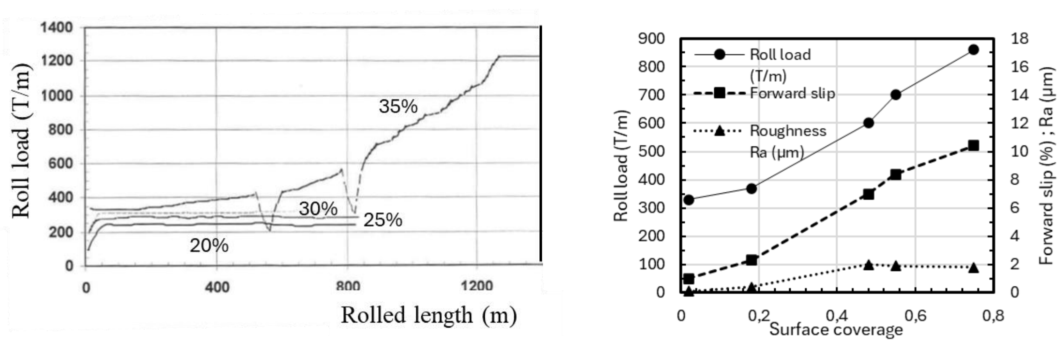


(a) (b)

**Figure 5**: Results from austenitic strip rolling, bright anneal, thickness 0.5 mm, at 5 m.s$^{-1}$; roll radius is 47 mm (after Rizoulières (2000)). (a) Evolution of roll load with rolled strip length for several reductions. (b) At 35% reduction, compared evolutions with coverage $\theta_{adh}$ of roll load, forward slip (strongly linked with friction) and strip roughness Ra (due to ploughing by the rough transfer layer areas on the roll)

Figure 5a shows the evolution of roll load with rolled length. Note the importance of the thickness reduction, with a clear threshold effect at 35%, i.e. largest surface expansion, pressure and above all temperature. This load increase occurs at constant roll speed and thickness reduction, proving that the cause is friction. In parallel, the formation of a thick and rough adhesive transfer layer on the roll has been observed, which ploughs scratches into the strip surface. Drops on the 35% curve are coil changes, which do not impact load evolution: this shows that the friction increase is due to roll surface evolution.

Figure 5b displays the evolutions of parameters linked with friction in the 35% case: roll load, forward slip (the best indicator of friction) and strip surface roughness Ra measured on strip samples taken after different rolled lengths, more or less the negative print of the roll roughness. All three are plotted versus the strip surface coverage by scratched areas corresponding to adhered areas on the roll; also measured on strip samples, it serves as an indirect quantification of adhesion.

The similar evolutions of roll load, forward slip and strip roughness are due to their common cause, growing adhesive transfer coverage of the roll. It may thus be concluded that as the transfer layer develops, friction increases due to the growth of a ploughing term. Based on these measurements, a linear relationship is assumed:

$$\mu(\theta_{adh}) = (1 - \theta_{adh}).\mu_0 + \theta_{cov}.\mu_{sat} \qquad (16)$$

i.e. friction coefficient is $\mu_0$ before onset of adhesion, when the rolls are smooth (Ra < 0.05 µm) and $\mu_{sat}$ when the rough adhesive transfer layer completely covers the roll surface (Ra = 1.5 – 2.0 µm).

# 4 Applications

## 4.1 Influence of major rolling parameters

Rolling of a ferritic stainless steel is taken as an example. The following stress ($\sigma$) - strain ($\varepsilon$) – temperature relationship is taken from Aperam's database:

$$\sigma\,(\frac{N}{mm2}) = 10(\frac{99.48}{T^{0.08}} + 11.512\varepsilon)(1 - 0.2e^{-2.7\varepsilon}) \qquad (17)$$

Roll speed varies between 50 and 600 m.min$^{-1}$, thickness reduction varies between 15 and 40%. Rigid steel roll diameter is 200 mm. Initial strip thickness is 2.32 mm. The composite roughness is $R_q$ = 1µm with a sawtooth geometry (pitch 12 µm) imprinted by the roll. Oil viscosity is given by

$$\eta = \eta_0 e^{\alpha p_b - \beta\Delta T} \qquad (18)$$

In this section, $\eta_0 = 0.01\ Pa.s, \alpha = 1.5\ 10^{-8}\ Pa^{-1}, \beta = 0.04\ K^{-1}$. The thermo-tribo-mechanical coupled model is applied (but adhesion is not triggered here). Figure 6a shows the effect of reduction (15-40%) on different parameters taken at bite exit. The fractional real area of contact $A_{out}$ increases while film thickness $h_{t,out}$ decreases; as a result, the friction coefficient $\mu$ averaged over the roll bite increases. In parallel, increasing reduction increases the friction flux entering the roll: bite exit roll surface temperature therefore increases from 65°C at 15% reduction to 180°C at 40%. The average lubricant temperature $T_{lub} = (T_{roll} + T_{strip})/2$ will naturally also increase with reduction.

Figure 6b shows the effect of roll speed (50-600 m/min, i.e. 0.83-10 m.s$^{-1}$). Increasing velocity, friction decreases, due to a smaller final area of contact $A$ and a higher film thickness $h_t$. It also leads to a slight decrease in temperature. This behaviour is explained by the increase in the Peclet number with rolling speed, which enhances advective heat transport along the roll surface and reduces the time available for radial heat diffusion towards the roll centre. This makes cooling by the lubricant more efficient. Note that the trend would be quite different in multipass rolling, because the strip would enter the roll bite at pass N with part of the heat accumulated during passes 1 to N-1; one generally observes a bell curve, due to heat accumulating as long as the strip is thick, but cooling becoming predominant for thinner gauges.

Figure 7 shows a Stribeck's curve, i.e. the evolution of friction over a larger roll speed range, showing the transition from the boundary to the mixed regime.

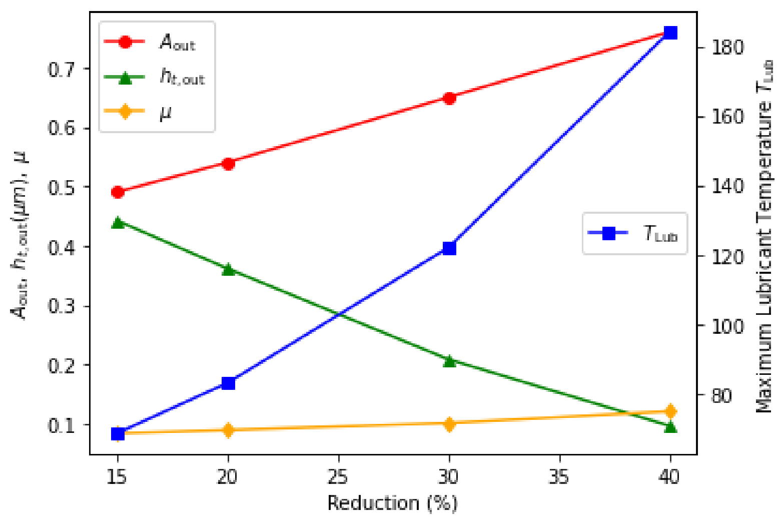


(a)

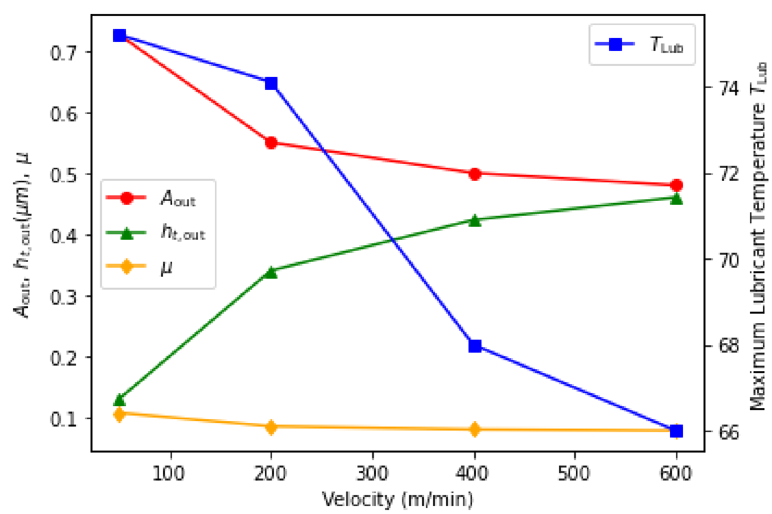


(b)

**Figure 6:** Effect of reduction and roll speed. Subscript "out" means "at bite exit".
(a) effect of reduction on the real area of contact $A$, the film thickness $h_t$ and the lubricant temperature $T_{lub}$ ($v_{roll}$ = 7.13 m.s$^{-1}$). (b) effect of roll speed (thickness reduction 15%).

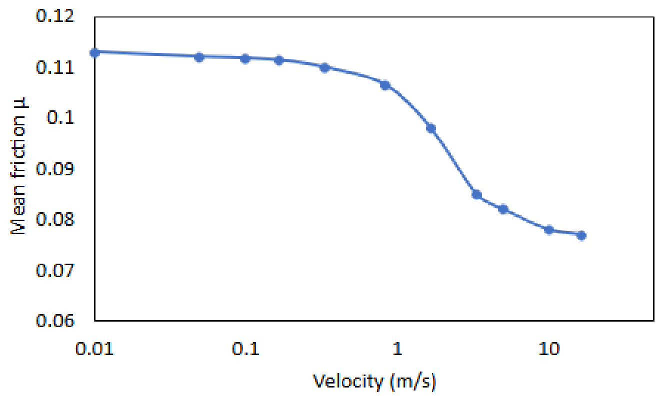


**Figure 7:** Effect of roll speed on average friction coefficient (Stribeck's curve). Thickness reduction is 15%.

## 4.2 Adhesion in stainless steel rolling and the resulting friction increase

The development of the adhesive transfer layer involves the following sequence of models:

1. The time-dependent roll thermal model is run for the duration of the rolling experiment (Figure 8). The roll surface starts at room temperature; the cycle (one revolution, Figure 8b) is composed of a short stage of cooling by the cold strip, then strip plastic deformation produces plastic and frictional heat, resulting in roll surface temperature growth; then the roll material point goes out of the bite and is cooled at different rates (air cooling, spray cooling, then air cooling again), to reach a steady temperature until next entry into the bite. As rolling proceeds, the whole curve moves up as the heat penetrates deeper and deeper towards the roll center.

2. At each cycle N (roll revolution), the part of the arc of contact is determined, over which the dual film thickness / temperature criterion is met (eq.(14), with $T_{crit}$ = 120°C). This may not be the case in the first roll revolutions but becomes true once the roll center has been warmed sufficiently.

3. Over this zone, eq.(15) is integrated and the new surface coverage $\theta_{adh}$(N+1) and the friction coefficient for next revolution is calculated accordingly (eq.(16)). $\mu_0$ and $\mu_{sat}$ have been selected to fit the experimental roll loads at the beginning (smooth roll) and the end (rough roll) of a test.

4. This procedure is repeated until completion of the rolling program (maximum number of revolutions) or until $\theta_{adh}$ = 1 because steady state is ensured beyond.

This procedure is illustrated in a case of bright annealed ferritic stainless-steel rolling, reported in (Rizoulieres 2000). Rolling speed is 5 m.s$^{-1}$, thickness reduction 30%. The stress-strain relationship is again given by eq.(17), the viscosity by eq.(18) with $\eta_0 = 0.007\ Pa.s, \alpha = 1.5\ 10^{-8}\ Pa^{-1}, \beta = 0.04\ K^{-1}$. Based on the data of (Rizoulieres 2000), the initial composite roughness $R_q$ = 0.044 µm. The roll-strip contact HTC is $h_{contact}$ = 0.45 MW.m$^{-2}$.K$^{-1}$.

An example of roll surface temperature evolution is plotted in Figure 8a. It takes two minutes to quasi-stabilize, due to the small roll diameter (94 mm). Figure 8b is an enlarged view of the roll surface temperature over one revolution in the stabilized state, reaching 130°C. Figure 8c shows that the final strip temperature is over 140°C due to the high friction.

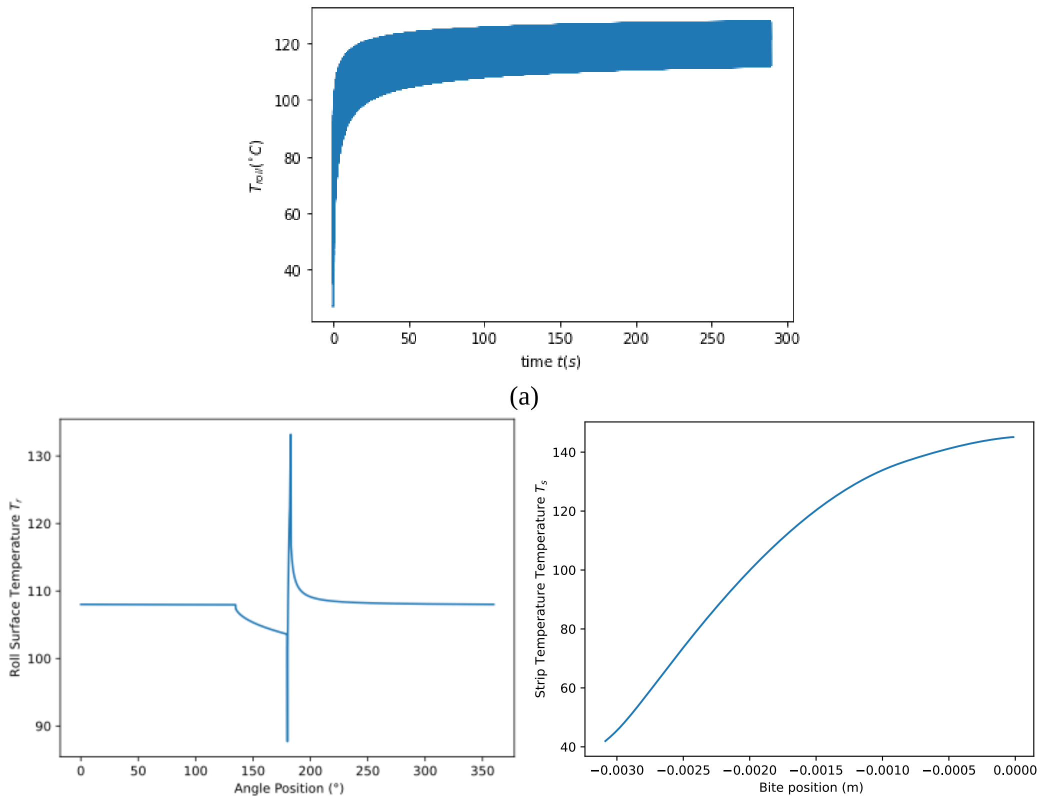


(b) (c)

**Figure 8**: (a) Time evolution of the computed roll surface temperature cycle. (b) Roll surface temperature profile when reaching steady state. (c) Strip temperature profile in the bite at the same stage. Ferritic stainless-steel rolling, 5 m.s$^{-1}$, thickness reduction 30%.

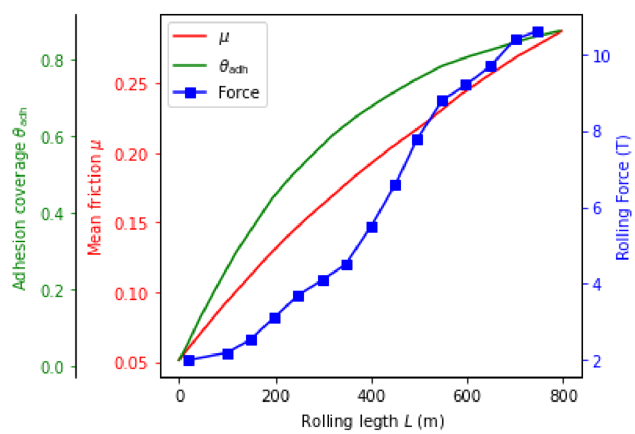


**Figure 9**: Consequences of the development of an adhesive transfer layer on the rolls, ferritic stainless-steel rolling, 5 m.s$^{-1}$ ($\mu_0 = 0.05, \mu_{sat} = 0.28\,; T_{crit} = 120°C$).

As strip and roll maximum (bite exit) temperatures grow along roll revolutions, the coverage rate $\theta_{adh}$ increases (Figure 9) and so does the friction coefficient (see equation(16)); as a consequence, the roll load increases from 2 to 10 Tons, at constant rolling conditions! Remember that these load values are experimental ones, fitted using $\mu_0$ and $\mu_{sat}$. The detailed comparison (not shown here) of the *shapes* of the $\theta_{adh}(L)$ and roll load curves shows some discrepancies: computation with eq.(15) does not reflect an inception time clearly visible in experiments (S-curves). This means that the adhesion mechanism inspired by Kitano et al. (2016) in eq.(15) needs to be adapted to this specific case of moderate, reversible adhesion rather than welding / seizure. This could e.g. by replacing the term 1-$\theta$ by $\theta$.(1-$\theta$) to represent a S-curve.

# 5 Conclusion and perspectives

Compared with previous mixed lubrication regime models, for which boundary friction remains an invariable fitting coefficient, the presented framework provides a capacity to implement a diversity of physically founded models. This has been made possible by the implementation of a coupled temperature model. Note that the ideas in Liu & Tieu (2002) who distinguish the lubricant temperature (which governs oil viscosity) and the boundary areas temperature (which concentrates the frictional heat) seem particularly interesting in view of accurately implementing physical-chemical models. This is left for future developments.

Indeed, the boundary friction model is applied here to adhesive transfer in the particular case of stainless steels. However, the same approach may be used, coupled with adsorption isotherms and computed temperatures and pressures, to predict the evolution of an adsorbed friction limiter boundary layer like fatty acids, alcohols or amines; it seems possible also to address anti-wear / extreme pressure additives, provided the pressure / shear stress / temperature / time film-formation models have been determined beforehand.

# References

Azushima, A. (1987). *Lubrication in steel strip rolling in Japan*. Trib. Int. 20, 6, 316-321

Boemer, D. (2020). *Numerical modeling of friction in lubricated cold rolling*. PhD Dissertation, University of Liège

Carretta, Y., Boman, R., Stephany, A., Legrand, N., Laugier, M., Ponthot, J.-P. (2011). *MetaLub - a slab method software for the numerical simulation of mixed lubrication regime in cold strip rolling*. Proc. Inst. Mech. Engrs J – J. Engg Trib 225, J9, 894-904

Hitchcock, J.H. (1935). *Roll neck bearings*. Report ASME Research Committee

Jacobs, L.J.M. (2025). *Modelling friction in cold rolling*. PhD Dissertation, University of Twente.

Johnson, K. L. (1987). *Contact mechanics*. Cambridge University Press.

Jortner, D., Osterle, J.F., Zorowski, C.F. (1960). *An analysis of cold strip rolling*. Int. J. Mech. Sci. 2, 3, 179-194

Kitano, H., Dohda, K., Ehmann, K.F. (2016). *Integrated adhesion model in dry forming and machining*. Proc. ICTMP 2016 (Phuket, Thailand, 2016), Thai Tribology Association, 80-87

Liu, Y.J., Tieu, A.K. (2002). *A thermal mixed film lubrication model in cold rolling*. J. Mat. Proc. Techn. 130-131, 202-207

Marsault N. (1998). *Modélisation du régime de lubrification mixte en laminage à froid (Modelling the mixed lubrication regime in cold rolling)*. Doctoral Dissertation, École des Mines de Paris (in French).

Mikic, B.B. (1974). *Thermal contact conductance: theoretical considerations*. Int. J. Heat Mass Transfer 17, 205-214

Montmitonnet, P., Delamare, F., Rizoulières, B. (2000). *Transfer layer and friction in cold metal strip rolling processes*. Wear 245, 125-135

Patir N., Cheng H.S. (1979). *Application of average flow model to lubrication between rough sliding surfaces*. ASME J. Lub. Tech. 101, 220–229

Patula, E. J. (1981). *Steady-State Temperature Distribution in a Rotating Roll Subject to Surface Heat Fluxes and Convective Cooling*. J. Heat Transf. 103, 1, 36–41

Qiu Z.L., Yuen W.Y.D., Tieu A.K. (1999). Mixed film lubrication theory and tension effects on metal rolling processes. ASME J. Trib. 121, 908–915

Rasp W., Häfele P. (1998). *Investigation into tribology of cold strip rolling*. Steel Res. 69, 4–5, 154–160

Rizoulières, B. (2000). *Couches de transfert et frottement en laminage à froid des aciers inoxydables (transfer layers and friction in cold rolling of stainless steel)*. PhD Dissertation, Ecole des Mines de Paris.

Sacadura, J.-F. (2015). *Transferts thermique - Initiation et approfondissements (Heat Transfer – From basics to advanced notions*. Tec & Doc, Lavoisier, Paris (in French).

Sheu S., Wilson W.R.D. (1994). *Mixed Lubrication of strip rolling*. STLE Trib. Trans. 37, 483–493

Sutcliffe M.P.F., Johnson K.L. (1990). *Lubrication in cold strip rolling in the mixed regime*. Proc. Instn. Mech. Engrs. 204, 249–261

Sutcliffe M.P.F. (1988). *Surface asperity deformation in metal forming processes*. Int. J. Mech. Sci. 30 (11) 847–868

Tsao Y.H., Sargent L.B. *A mixed lubrication model for the cold rolling of metals*. ASLE Trans. 20 (1977) 55–63

Tseng, A.A. (1999). *Thermal modeling of roll and strip interface in rolling processes: part 2-simulation*. Numer. Heat Transf. Part Appl. 35, 2, 135–154

Von Karman, T. (1925). *Beitrag zur Theorie des Walzvorganges*. ZAMM 5 (1925) 139–141

Wilson, W.R.D., Marsault, N. (1998). *Partial hydrodynamic lubrication with large fractional contact areas*. ASME J. Trib. 120, 1, 16-20

Wilson W.R.D., Sheu S. (1988). *Real area of contact and boundary friction in metal forming*. Int. J. Mech. Sci. 30 (7) 475–489

Wu J.Q., Liang X.P., Tang A.T., Pan F.S. (2016) *Interfacial heat transfer under mixed lubrication condition for metal rolling: a theoretical calculation study*. Appl. Therm. Engg 106, 1002-1009